Cell Reports
Methods

Report

Tau^{LUM}, an *in vivo Drosophila* sensor of tau multimerization, identifies neuroprotective interventions in tauopathy

Graphical abstract

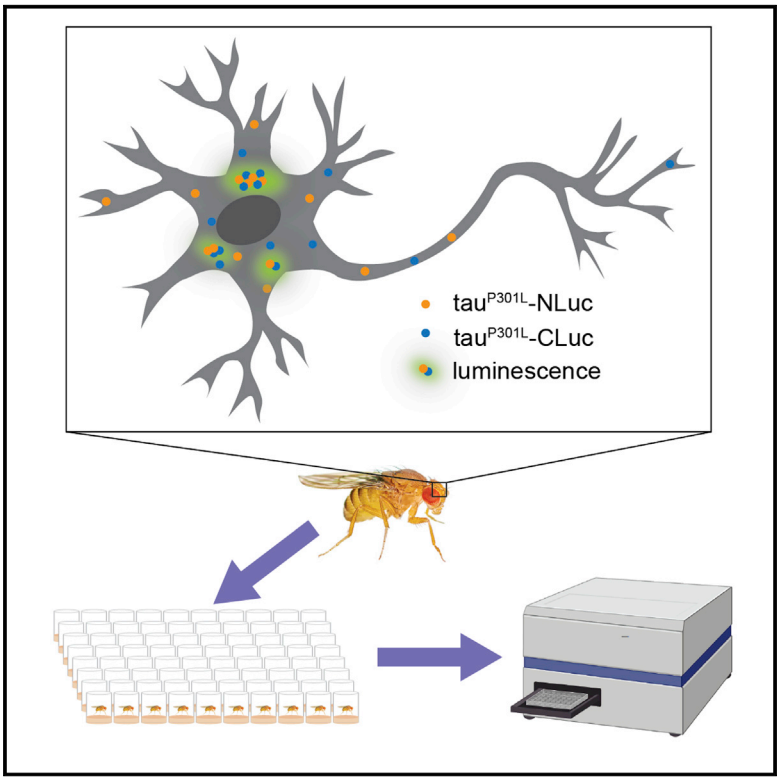

Highlights

- Tau^{LUM} is a luminescence-based *Drosophila* model of tau multimerization
- Tau^{LUM} can measure tau multimerization *in vivo* at single time points or longitudinally
- Tau^{LUM} identifies small-molecule and genetic modifiers of tau multimerization

Authors

Simon A. Levy, Gabrielle Zuniga, Elias M. Gonzalez, David Butler, Sally Temple, Bess Frost

Correspondence

bfrost@uthscsa.edu

In brief

Tau multimerization is a core pathological feature of many neurodegenerative disorders, including Alzheimer's disease. Here, Levy et al. present tau^{LUM}, a *Drosophila* model that leverages split-luciferase technology to assay tau multimerization *in vivo*. Tau^{LUM} is a powerful discovery platform for identifying genetic regulators and drugs targeting tau multimerization.

Levy et al., 2022, Cell Reports Methods *2*, 100292
September 19, 2022
https://doi.org/10.1016/j.crmeth.2022.100292

CellPress

Cell Reports Methods

CellPress
OPEN ACCESS

Report

Tau^{LUM}, an *in vivo Drosophila* sensor of tau multimerization, identifies neuroprotective interventions in tauopathy

Simon A. Levy,[1,2,3] Gabrielle Zuniga,[1,2,3] Elias M. Gonzalez,[1,2,3] David Butler,[4] Sally Temple,[4] and Bess Frost[1,2,3,5,*]
[1]Barshop Institute for Longevity and Aging Studies, University of Texas Health San Antonio, San Antonio, TX 78229, USA
[2]Glenn Biggs Institute for Alzheimer's and Neurodegenerative Diseases, University of Texas Health San Antonio, San Antonio, TX 78229, USA
[3]Department of Cell Systems and Anatomy, University of Texas Health San Antonio, San Antonio, TX 78229, USA
[4]Neural Stem Cell Institute, Rensselaer, NY 12144, USA
[5]Lead contact
*Correspondence: bfrost@uthscsa.edu
https://doi.org/10.1016/j.crmeth.2022.100292

MOTIVATION Deposition of tau into fibrillar aggregates is a core feature of Alzheimer's disease and related tauopathies. However, current systems to investigate tau multimerization are based on artificial cell culture systems or rely on analyses of postmortem rodent brain tissue. To overcome these limitations and elucidate the mechanisms that mediate tau multimerization, we present tau^{LUM}, a luminescence-based *Drosophila* sensor of tau multimerization capable of longitudinal measurements in a living, aging brain.

SUMMARY

Tau protein aggregates are a defining neuropathological feature of "tauopathies," a group of neurodegenerative disorders that include Alzheimer's disease. In the current study, we develop a *Drosophila* split-luciferase-based sensor of tau-tau interaction. This model, which we term "tau^{LUM}," allows investigators to quantify tau multimerization at individual time points or longitudinally in adult, living animals housed in a 96-well plate. Tau^{LUM} causes cell death in the adult *Drosophila* brain and responds to both pharmacological and genetic interventions. We find that transgenic expression of an anti-tau intrabody or pharmacological inhibition of HSP90 reduces tau multimerization and cell death in tau^{LUM} flies, establishing the suitability of this system for future drug and genetic modifier screening. Overall, our studies position tau^{LUM} as a powerful *in vivo* discovery platform that leverages the advantages of the *Drosophila* model organism to better understand tau multimerization.

INTRODUCTION

The deposition of tau into fibrillar aggregates is a hallmark of a host of neurodegenerative diseases, which include Alzheimer's disease, collectively termed "tauopathies" (Arendt et al., 2016). A prevailing hypothesis to explain the stereotypical temporal pattern of tau deposition in Alzheimer's disease (Braak and Braak, 1991; Braak et al., 2011) is the prion hypothesis, which posits that small, mobile multimeric tau seeds propagate misfolding of native tau between cells (Frost and Diamond, 2010). While the prion hypothesis of tauopathy has been validated in various systems (Clavaguera et al., 2009; Frost et al., 2009a, 2009b; Vaquer-Alicea and Diamond, 2019), the initial steps that lead to the formation of pathogenic tau seeds are still incompletely understood.

A barrier to gaining better insight into the biological underpinnings of tau multimerization and to developing strategies to target this process is the difficulty of quantifying active tau multimerization in a living animal. Current *in vivo* approaches rely mainly on single time points with postmortem analyses of brain tissue using either histology or western blotting. Current cell-based approaches typically rely on monocultures that do not accurately model the myriad cell types in a living brain and often utilize cell types that are not present in the brain. There is a need for *in vivo* platforms that enable us to measure tau multimerization in a living, aging brain and to examine the dynamics of tau multimerization over time. Biochemically, protein-protein interaction lies at the core of tau multimerization and, as such, can be measured using techniques aimed at detecting protein-protein interactions. Split-protein complementation assays are a set of such techniques that include split-luciferase assays as well as fluorescence-based approaches (Villalobos et al., 2007). Split-luciferase assays are based on the concept that fragments of the luciferase enzyme can recover partial activity

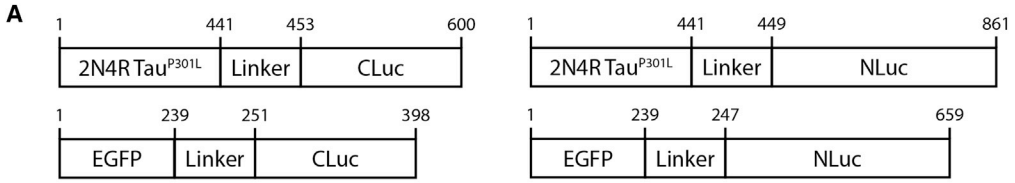

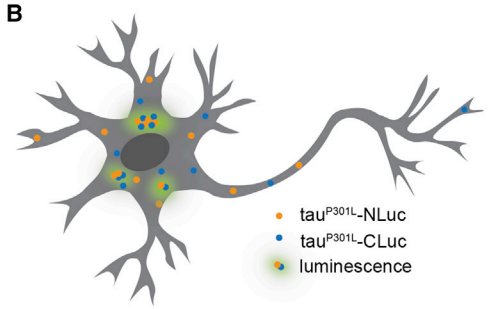

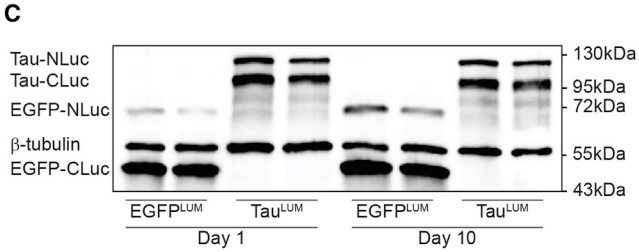

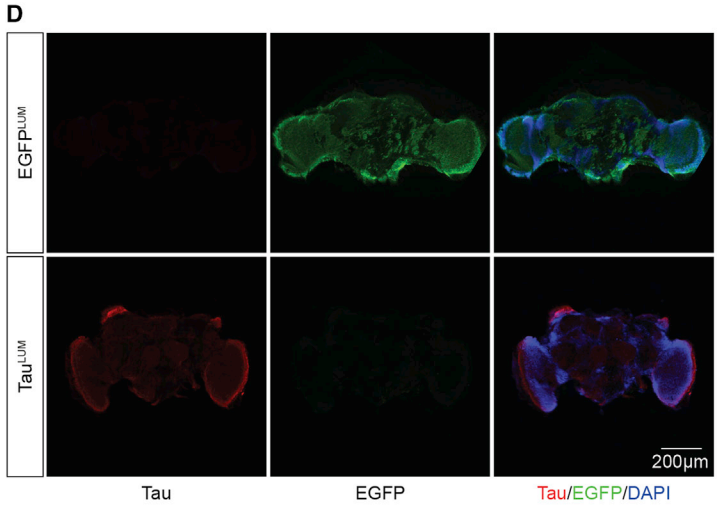

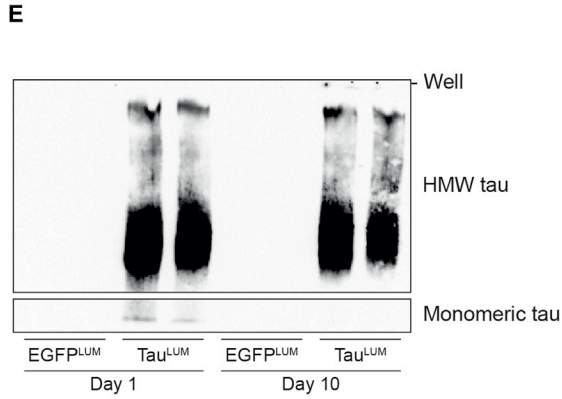

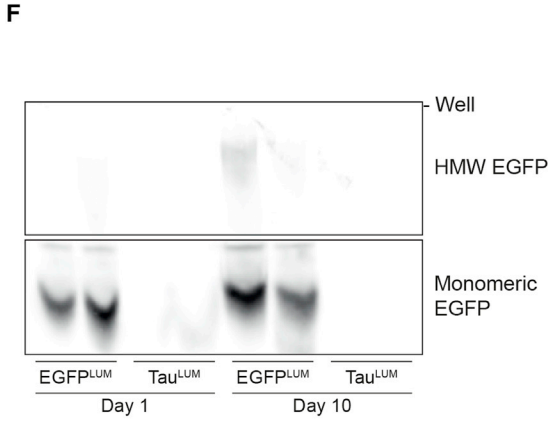

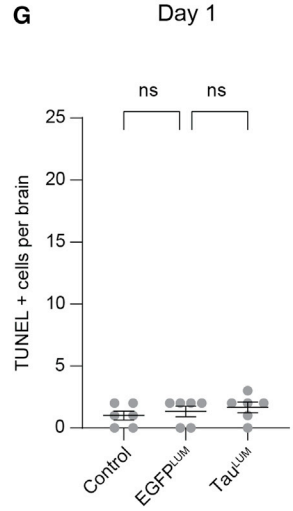

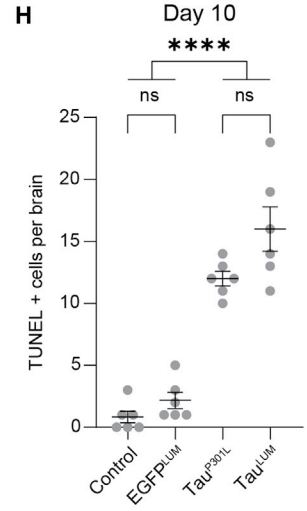

(legend on next page)

and emit bioluminescence when brought into close proximity to one another and supplied with D-Luciferin as a substrate. They have been used to quantify protein-protein interactions both in cell culture and *in vivo* (Naik and Piwnica-Worms, 2007).

Building upon previous work utilizing a split-luciferase approach to detect tau-tau interactions in cultured cells (Sanders et al., 2014), we have developed an *in vivo* platform to quantify tau multimerization in the adult *Drosophila* brain. Our model, which we name tau^{LUM}, provides a readout of tau multimerization and responds to both pharmacological and genetic interventions. Performing these studies in a living, aging *Drosophila* brain allows experiments investigating aging-related processes, as aging is the greatest risk factor for tauopathies.

RESULTS

Tau^{LUM} is expressed in neurons and causes cell death in the adult *Drosophila* brain

We created *Drosophila* that transgenically express the disease-associated (Hutton et al., 1998; Lewis et al., 2000) *P301L* variant of full-length 2N4R human *MAPT*, hereafter referred to as "tau," fused to either the C-terminal (CLuc) or N-terminal (NLuc) portion of the luciferase enzyme (Figure 1A). In these flies, which we refer to as tau^{LUM}, multimerization of tau protein brings the NLuc and CLuc fragments together and allows them to emit bioluminescence in the presence of the luciferase substrate D-Luciferin (Figure 1B). We also created a non-multimerizing genetic control for the tau^{LUM} system, which we term EGFP^{LUM}. This control system features fusion of the NLuc and CLuc fragments to transgenic EGFP rather than transgenic tau (Figure 1A). Both tau^{LUM} and EGFP^{LUM} were created using site-directed integration of transgenes into the same location within the *Drosophila* genome to control for any positional effects of gene insertion. All transgenes are expressed pan-neuronally using the *elav-Gal4* promoter.

Based on western blotting, we observe robust expression of tau^{P301L}-CLuc, tau^{P301L}-NLuc, EGFP-CLuc, and EGFP-NLuc fusion proteins in *Drosophila* heads at days 1 and 10 of adulthood (Figure 1C). The lower intensity of NLuc fusion protein bands compared with CLuc is likely due to positional effects of transgene insertion sites. Additionally, immunofluorescence-based detection of tau and EGFP in 1-day-old tau^{LUM} and EGFP^{LUM} flies shows widespread expression of transgenes in *Drosophila* neurons (Figure 1D). We next asked whether the transgenic tau in tau^{LUM} forms multimeric species. Native gel electrophoresis performed without SDS to preserve quaternary structure revealed a smear of high molecular weight tau species (Figure 1E), indicative of multimerization at both 1 and 10 days of age. EGFP^{LUM} flies did not exhibit a high molecular weight smear and only had very faint signal outside of the monomeric bands (Figure 1F). As proteins are not linearized in SDS-free conditions, exact molecular weights of the various protein species cannot be determined with this technique.

While we do not detect significant levels of cell death in tau^{LUM} or EGFP^{LUM} at day 1 of adulthood based on terminal deoxynucleotidyl transferase dUTP nick end labeling (TUNEL) (Figure 1G), we find that TUNEL-positive cells are significantly increased in tau^{LUM} *Drosophila* compared with EGFP^{LUM} by day 10 of adulthood (Figure 1H), indicating that the transgenic tau protein has toxic consequences for the *Drosophila* brain that manifest progressively with age. The amount of neurodegeneration observed in tau^{LUM} flies is comparable to that of flies pan-neuronally expressing tau^{P301L} alone (Figure 1H). We observe similarly increased levels of neurotoxicity in tau^{LUM} animals compared with EGFP^{LUM} controls when quantifying vacuoles in the *Drosophila* brain (Figure S1). Taken together, these data show that tau^{LUM} and EGFP^{LUM} *Drosophila* models have robust expression of their constituent transgenes, that tau, but not EGFP, forms high molecular weight species in the *Drosophila* brain, and that transgenic overexpression of tau protein in tau^{LUM} leads to progressive cell death.

Luminescence-based quantification of tau multimerization in live tau^{LUM} flies

Having demonstrated that the components of the tau^{LUM} and EGFP^{LUM} systems are expressed as expected and that tau^{LUM} causes neurotoxicity in the *Drosophila* brain, we next investigated whether the tau^{LUM} model can be used to measure tau multimerization via bioluminescence. A major advantage of a bioluminescence-based platform such as tau^{LUM} is that signal can be acquired from live animals. After being placed on food enriched with D-Luciferin, the substrate for luciferase, the animals were individually placed into wells of a 96-well plate (Figure 2A) at least 30 min prior to signal acquisition in a plate reader. At both 1 and 10 days of age, tau^{LUM} *Drosophila* exhibited significantly higher luminescence signal than EGFP^{LUM} control animals (Figures 2B and 2C). The difference in luminescence between tau^{LUM} and EGFP^{LUM} is approximately 0.7 on the logarithmic scale, which corresponds to a linear difference on the order of 5-fold. Importantly, none of the constituent transgenes of tau^{LUM} or EGFP^{LUM} emitted luminescence above that of a wild-type fly when expressed alone, indicating that luminescence emission

Figure 1. Tau^{LUM} and EGFP^{LUM} systems

(A) Gene models of the transgenes used for tau^{LUM} and EGFP^{LUM} systems.
(B) Schematic overview of the tau^{LUM} system.
(C) Protein expression in EGFP^{LUM} and tau^{LUM} flies at 1 and 10 days of age by western blotting.
(D) Tau and EGFP protein expression in EGFP^{LUM} and tau^{LUM} flies at 1 day of age based on immunofluorescence.
(E) Native gel blotting reveals high molecular weight smear in tau^{LUM} *Drosophila* at 1 and 10 days of age.
(F) EGFP^{LUM} flies do not exhibit significant EGFP multimerization.
(G) Low levels of cell death in 1-day-old tau^{LUM} and EGFP^{LUM} *Drosophila* assayed by TUNEL staining.
(H) Increased levels of cell death in 10-day-old tau^{LUM} flies compared with EGFP^{LUM}.
(G and H) n = 6 per group. Data are presented as mean ± SEM. (G) One-way ANOVA with Dunnett's post-hoc test. (H) One-way ANOVA with Tukey's post-hoc test. ****$p < 0.0001$.

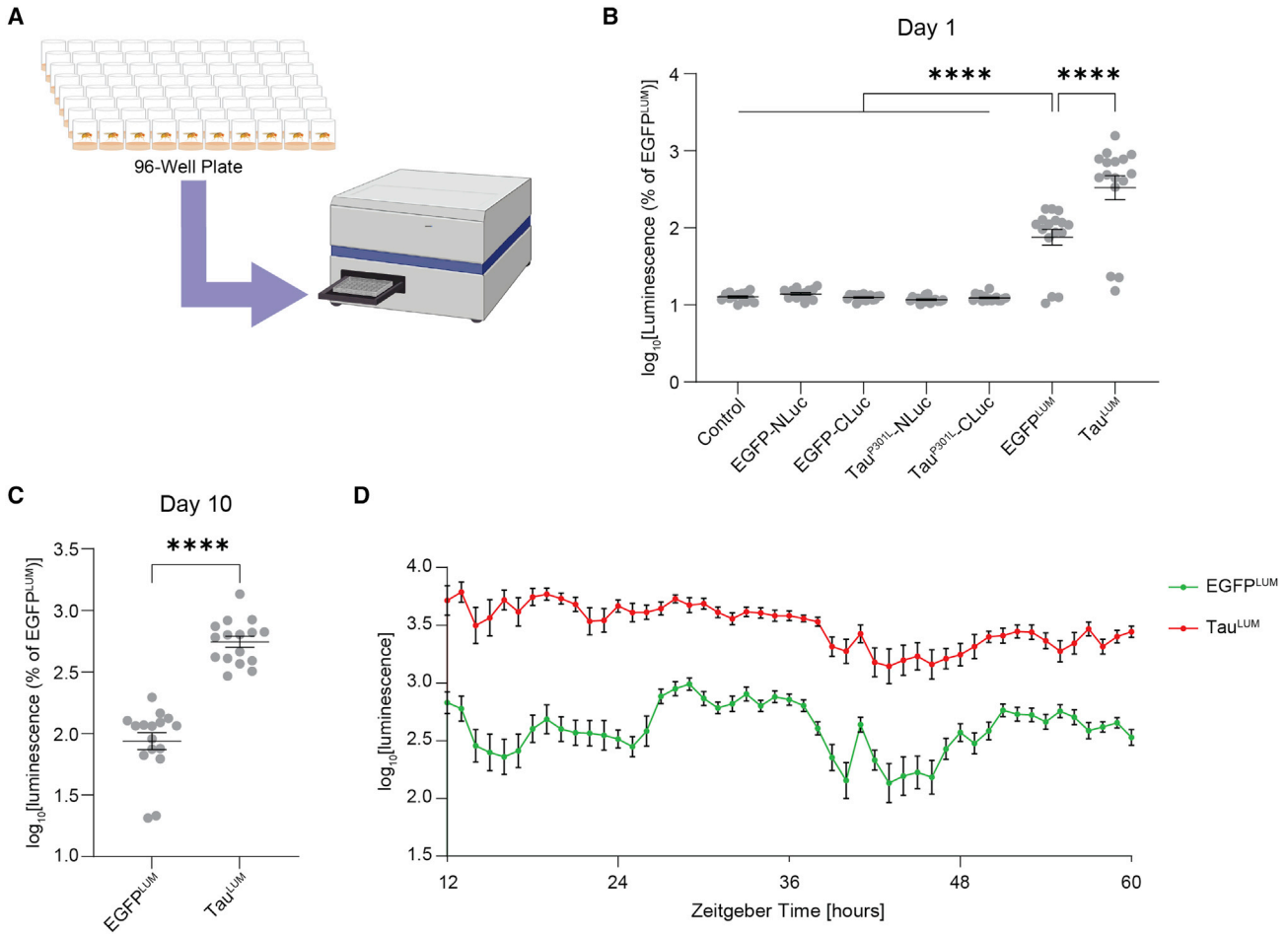

Figure 2. Quantifying tau multimerization by luminescence

(A) Schematic overview of luminescence experimental setup.

(B and C) Luminescence measurements of EGFP^{LUM} and tau^{LUM} flies at 1 (B) and 10 (C) days of age by plate reader.

(D) Longitudinal measurements of luminescence in EGFP^{LUM} and tau^{LUM} flies by plate reader.

(B–D) n = 16 per group. Data are presented as mean ± SEM. One-way ANOVA with Dunnett's post-hoc test (B) and Student's two-tailed unpaired t test (C). ****$p < 0.0001$.

is specific to protein-protein interaction between NLuc and CLuc fusion proteins (Figure 2B). When normalized to the signal from sex-matched EGFP^{LUM} controls, two-way ANOVA reveals no main effect of sex on the luminescence signal from tau^{LUM} *Drosophila* at either 1 or 10 days of age, indicating that sex is not a confounding variable for the tau^{LUM} system (Figure S2).

Since luminescence can be acquired from live *Drosophila*, we also tested whether tau^{LUM} was amenable to quantifying tau multimerization over time. After placing the animals into wells of a 96-well plate containing food fortified with D-Luciferin, the luminescence signal was acquired every hour for 2 days (Figure 2D). We find that the luminescence signal can be stably acquired over multiple days using this approach and that tau^{LUM} flies consistently emit a higher signal than EGFP^{LUM} control animals. In summary, tau multimerization can be quantified in tau^{LUM} *Drosophila* via bioluminescence *in vivo* either at single time points or repeatedly over time. We find that increased bioluminescence in tau^{LUM} flies precedes increased levels of cell death observed at 10 days of age.

Anti-tau intrabodies reduce tau^{LUM} luminescence and cell death

One of the major strengths of *Drosophila* as a model organism is its extensive genetic toolkit and the ease with which potential genetic modifiers can be introduced. We next took a genetic approach to assess whether the tau^{LUM} luminescence signal responds to interventions targeting tau multimerization. Intrabodies are transgenically expressed custom antibodies that have been used previously to target huntingtin aggregation (Wolfgang et al., 2005) and tau toxicity (Krishnaswamy et al., 2020) in *Drosophila* models. Co-expression of tau^{LUM} with an anti-tau intrabody recognizing amino acids 368–391 (Visintin et al., 2002) (Figures 3A and 3B) significantly reduces luminescence-based detection of tau multimerization in 1-day-old *Drosophila*

CellPress
OPEN ACCESS

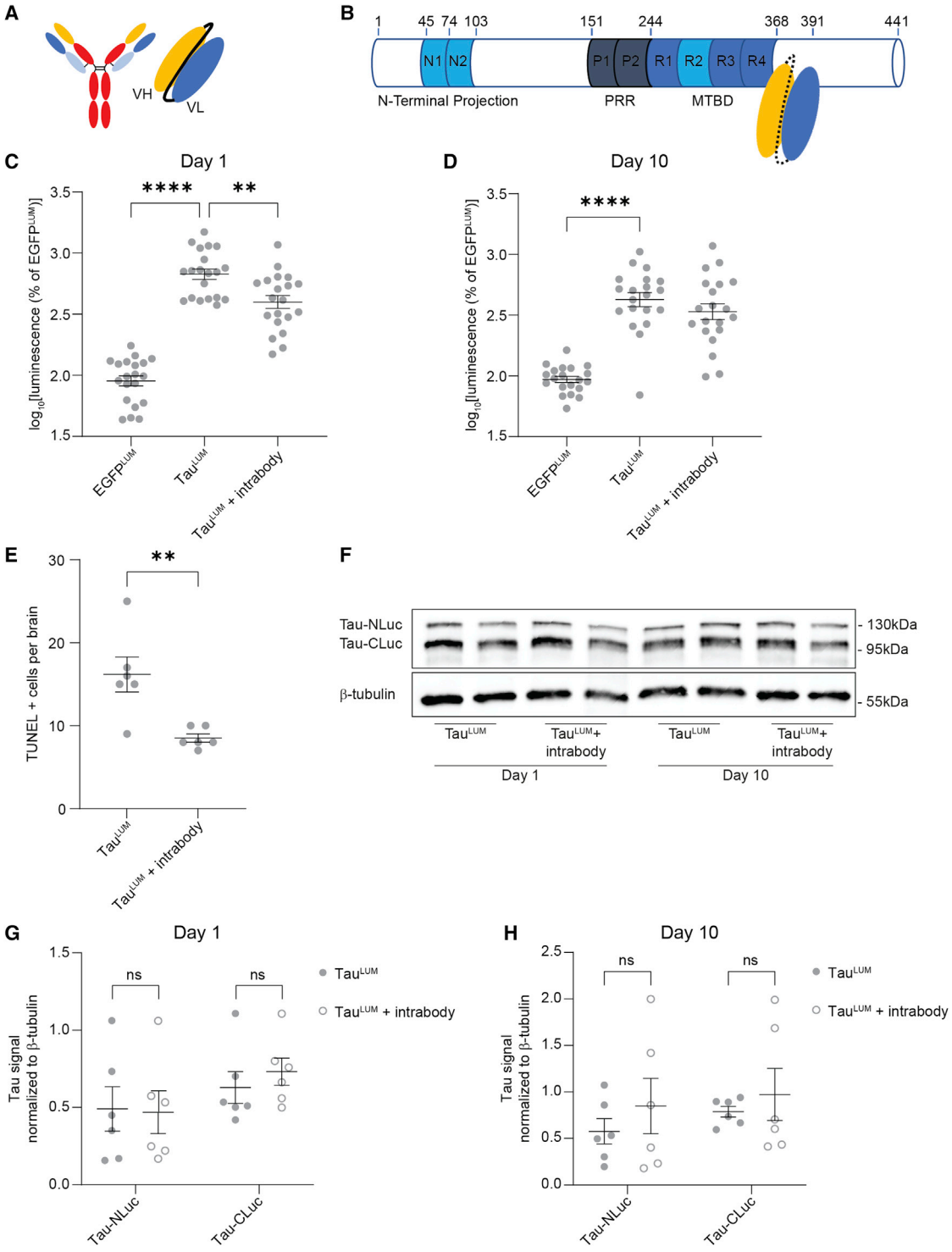

Figure 3. Anti-tau intrabodies reduce tau multimerization

(A) Recombinant intracellular antibodies, or intrabodies, contain the variable heavy (VH) and variable light (VL) antigen binding domains of conventional full-length antibodies. Red, light blue, yellow, and dark blue areas represent constant heavy, constant light, VH, and VL domains, respectively.

(B) Anti-tau intrabody was selected against amino acids 151–441, which contain proline-rich regions (RPPs) and microtubule-binding domains (MTBDs). The intrabody recognizes an epitope residing within amino acids 368–391.

(C) Decreased tau^{LUM} luminescence with anti-tau intrabody in 1-day-old flies.

(legend continued on next page)

(Figure 3C). Intriguingly, the effect of the tau intrabody on tau multimerization is no longer present at day 10 of adulthood (Figure 3D), suggesting that tau multimerization overcomes the barrier posed by intrabody interference given enough time. We find reduced cell death in brains of tau^{LUM} animals co-expressing the intrabody at 10 days of age (Figure 3E), indicating that the early effects of the intrabody are sufficient to reduce toxicity later in adulthood. The tau intrabody is not coupled to a degradation signal and was thus not expected to alter overall transgenic tau protein levels. Indeed, we do not observe changes in tau-NLuc or tau-CLuc levels at either 1 or 10 days of age upon co-expression of the anti-tau intrabody (Figures 3F–3H), suggesting that changes in luminescence reflect altered tau-tau interaction rather than a simple reduction in tau protein levels.

Inhibition of the molecular chaperone HSP90 reduces tau multimerization and cell death in tau^{LUM}

In addition to the ease of genetic manipulation, *Drosophila* are well suited for pharmacological screening, as drug candidates can be administered by simply mixing them into the food. Our next step was to thus test whether tau^{LUM} activation responds to pharmacological intervention. Tau is a client protein of the molecular chaperone HSP90 (Karagöz et al., 2014), which aids in the folding of tau. We tested whether radicicol, a macrocyclic antibiotic inhibitor of HSP90 (Beljanski, 2007), changes tau multimerization as measured by tau^{LUM} luminescence. After 1 day of treatment, we did not detect a significant change in tau^{LUM} luminescence (Figure 4A). After 10 days of treatment, however, the tau^{LUM} signal in radicicol-treated *Drosophila* was significantly reduced compared with control animals (Figure 4B). Concurrent with the decrease in luminescence, we also found reduced cell death in the brains of 10-day-old tau^{LUM} animals after HSP90 inhibition (Figure 4C). As with the genetic intervention described above, radicicol treatment does not significantly alter tau protein levels at either time point (Figures 4D–4F), indicating that the radicicol-induced decrease in luminescence reflects a change in tau-tau interaction. To verify that the difference in luminescence between vehicle- and radicicol-treated tau^{LUM} *Drosophila* is not due to changes in available substrate because of altered feeding, we placed tau^{LUM} animals on food containing blue dye and measured food intake by absorbance (Figure S3). We observed no difference in food intake between *Drosophila* fed vehicle or radicicol, indicating that luminescence differences reflect changes in tau-tau interaction. Taken together, these data indicate that the tau^{LUM} system provides a quantitative measure of tau-tau interaction *in vivo* that can be modulated by genetic or pharmacological interventions targeting tau to identify new avenues to reduce tau-induced cell death.

DISCUSSION

In this study, we present tau^{LUM}, an *in vivo* biosensor of tau multimerization. Based on transgenic expression of a split-luciferase system, tau^{LUM} is able to quantitatively detect tau-tau interaction and provide an *in vivo* luminescence readout that can be measured via plate reader at single time points or over multiple days. Our studies show that the tau^{LUM} signal rises above background levels produced by simply overexpressing a soluble protein fused to a split-luciferase system in neurons, as tau^{LUM} *Drosophila* emit a 5-fold increase in luminescence compared with EGFP^{LUM} control animals. We further show that split-luciferase components have negligible levels of background luminescence that do not differ from those of wild-type flies.

It is important to note that while tau^{LUM} provides a readout of overall tau multimerization, the system is agnostic regarding the exact nature of multimeric tau. Tau can adopt a range of multimeric species, ranging from dimers and trimers to larger oligomers and filamentous insoluble aggregates (Patterson et al., 2011). All of these types of multimers would be detectable using split-luciferase assays and should be captured by tau^{LUM}. Of note, split-luciferase interactions are reversible and thus do not produce artifacts by artificially stabilizing tau-tau interactions.

In its current form, the tau^{LUM} system utilizes the P301L tau mutant. This form of tau has previously been shown to be highly prone to multimerization and seeding of aggregation (Von Bergen et al., 2001; Guo and Lee, 2011; Strang et al., 2017). While wild-type tau exhibited less multimerization potential than P301L tau in these studies, many tauopathies, including Alzheimer's disease, primarily feature aggregates of wild-type tau. The transgene-linker-luciferase structure of tau^{LUM} transgenes makes the design of transgene sequences for future tau^{LUM} versions straightforward and will allow future work to investigate the differences in multimerization between different tau isoforms and mutant using the tau^{LUM} platform. Furthermore, the modular nature of *Drosophila* genetics will make it simple to investigate non-neuronal tauopathies by using different genetic driver lines to achieve expression of the tau^{LUM} system in glia or other cell types of interest.

As expected, we find elevated numbers of TUNEL-positive cells in the brains of tau^{LUM} flies compared with controls, indicating that transgenic expression of the P301L disease-associated tau mutation causes cell death in *Drosophila*. The level of cell death detected in tau^{LUM} *Drosophila* is comparable to that of flies pan-neuronally expressing tau^{P301L} not fused to luciferase fragments. This finding is consistent with observations in other *Drosophila* models expressing mutant or wild-type tau in neurons, which exhibit neurodegeneration to varying degrees (Wittmann et al., 2001; Bardai et al., 2018).

(D) No change in tau^{LUM} luminescence with anti-tau intrabody in 10-day old flies.
(E) Decreased levels of cell death in tau^{LUM} brains expressing anti-tau intrabodies at 10 days of age.
(F) Tau protein levels in tau^{LUM} with or without anti-tau intrabody at 1 or 10 days of age by western blotting.
(G and H) Quantification of western blotting data reveals no change in tau protein levels at 1 (G) or 10 (H) days of age.
(C and D) n = 20 per group; (E, G, and H) n = 6 per group. Data are presented as mean ± SEM.
(C and D) One-way ANOVA with Dunnett's post-hoc test.
(E) Unpaired two-tailed Student's t test.
(G and H) Two-way ANOVA with Sidak's multiple comparisons post-hoc test. **$p < 0.01$, ****$p < 0.0001$.

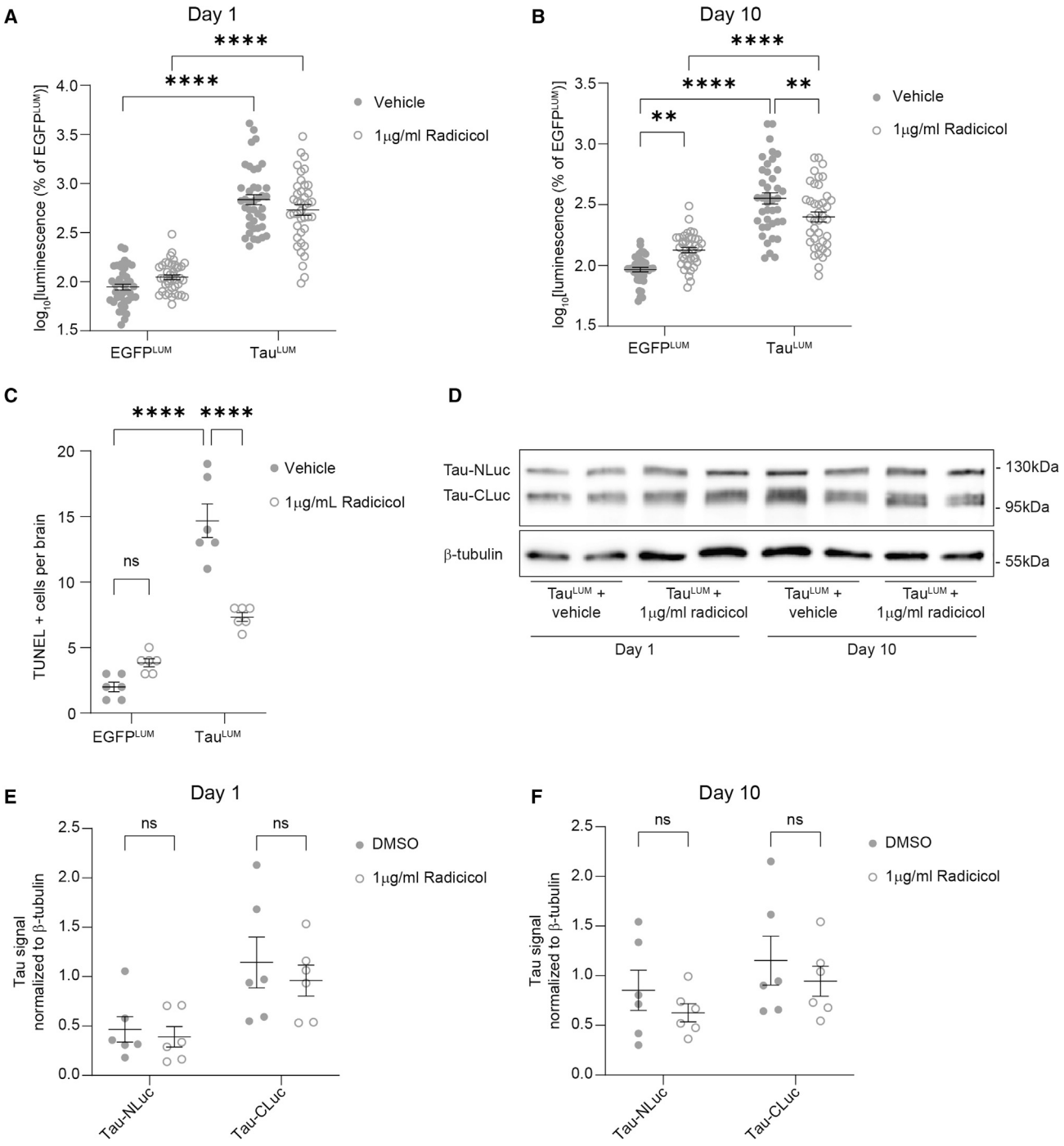

Figure 4. HSP90 inhibition reduces tau multimerization

(A) No significant change in tau^{LUM} luminescence after 24 h of radicicol treatment.

(B) Decreased tau^{LUM} luminescence after 10 days of HSP90 inhibition.

(C) Reduced levels of cell death in tau^{LUM} brains after 10 days of HSP90 inhibition.

(D) Tau protein levels in tau^{LUM} animals exposed to either vehicle (0.01% DMSO) or 1 μg/mL radicicol at 1 and 10 days of age by western blotting.

(E and F) Quantification of western blotting data reveals no change in tau protein levels at 1 (E) or 10 (F) days of age.

(A and B) n = 40 per group; (C, E, and F) n = 6 per group. Data are represented as mean ± SEM.

(A–C) Two-way ANOVA with Tukey's post-hoc test.

(E and F) Two-way ANOVA with Sidak's multiple comparisons post-hoc test. **p < 0.01, ***p < 0.001, ****p < 0.0001.

A major advantage of *Drosophila* as a model organism is the relative ease of genetic and pharmacological interventions. The large toolkit available for *Drosophila* genetics allows for the introduction of modifier genes into a model system. In addition, drugs can be delivered to fruit flies by simply mixing them into food. In order to validate the potential of tau^{LUM} as a platform for future discovery of novel regulators and modifiers of tau multimerization, we tested both genetic and pharmacological interventions of tau multimerization and quantified changes in the tau^{LUM} signal. We first employed an anti-tau intrabody approach to genetically interfere with tau-tau interaction. The anti-tau intrabody was transgenically expressed in neurons along with the constituent proteins of the tau^{LUM} system. The intrabody design was based on previous work using an anti-huntingtin intrabody to inhibit huntingtin aggregation in *Drosophila* (Wolfgang et al., 2005), which ameliorated huntingtin-associated disease phenotypes. We found a decrease in tau^{LUM} luminescence in 1-day-old flies upon co-expression of the anti-tau intrabody, consistent with decreased tau multimerization. However, this effect did not persist through day 10 of adulthood, indicating that the intrabody-mediated interference of tau-tau interactions can be overcome given enough time. We nevertheless find decreased levels of cell death in intrabody-expressing flies at day 10 of adulthood, which suggests that the intrabody's early effects on tau positively impact cell viability later in adulthood. Since the intrabody used in this study is not fused to a degradation signal that would target tau to the proteasome or lysosome, the most likely mechanism by which it interferes with tau multimerization is steric hindrance upon associating with tau protein.

We next tested inhibition of HSP90 as a pharmacological intervention. HSP90 has been shown to promote tau multimerization *in vitro* (Weickert et al., 2020). *In vivo* activation of HSP90 leads to increased deposition of hyperphosphorylated and oligomeric tau in mice (Criado-Marrero et al., 2021), as well as a decrease in the number of hippocampal neurons (Shelton et al., 2017). Inhibition of HSP90 in mice has further been reported to mitigate the effects of mutant, but not wild-type, tau (Luo et al., 2007). We would therefore expect inhibition of HSP90 to reduce tau multimerization and lower tau^{LUM} luminescence, which we observe after 10 days of HSP90 inhibition, along with a reduction in cell death. The presence of a non-significant trend toward lower tau^{LUM} luminescence after 1 day of inhibition suggests that the effects of HSP90 inhibition occur on a time scale of several days. Overall, we show that the tau^{LUM} system is able to quantify the impacts of both genetic and pharmacological interventions targeting tau or regulators of tau multimerization.

Taken together, our findings showcase the potential of the tau^{LUM} system as a discovery platform to investigate the biological underpinnings of tau multimerization. Tau^{LUM} provides a quantitative, *in vivo* readout of tau-tau interaction that can be acquired at single time points or longitudinally. Furthermore, we use tau^{LUM} to identify two interventions to modulate tau multimerization and lower cell death that leverage two main advantages of the *Drosophila* model organism, namely the ease of drug delivery and the introduction of genetic modifiers to the system. In both cases, tau^{LUM} is able to quantify the impact of the modifiers and identify differential effects at two distinct time points. The ability to acquire longitudinal measurements also allows the examination of dynamic processes. When combined with the rapid generational turnover and short lifespan of *Drosophila*, tau^{LUM} is an excellent platform to leverage into future medium-throughput screens of genetic modifiers and pharmacological inhibitors of tau multimerization.

Limitations of the study

The genetic framework we present allows the investigation of tau multimerization in living *Drosophila* through a luminescence readout. This method is ideally suited for examining the effects of pharmacological and genetic interventions on tau-tau interaction. However, the throughput of the tau^{LUM} system is limited by two factors: first, the need to manually insert flies into the wells of a 96-well plate prior to measurement, and second, the need to have sufficient numbers of flies at the appropriate age and of all experimental groups available on the day of measurement. This means that careful planning of *Drosophila* crosses is required. While the throughput of tau^{LUM} remains high compared with other *in vivo* systems and constitutes a net asset to the system—assaying a full 96-well plate of *Drosophila* is entirely feasible in one experiment—analyzing many different genotypes and treatment groups in sufficient numbers in a single experiment can become technically challenging due to the above constraints. A consideration for longitudinal luminescence measurements is that *Drosophila* food inside 96-well plates may be a limiting factor for how long an experiment may last. It is necessary to monitor the health of the animals in the plate periodically to ensure their continued access to food and to appropriately exclude animals from analysis should they die prematurely.

STAR★METHODS

Detailed methods are provided in the online version of this paper and include the following:

- KEY RESOURCES TABLE
- RESOURCE AVAILABILITY
  - Lead contact
  - Materials availability
  - Data and code availability
- EXPERIMENTAL MODEL AND SUBJECT DETAILS
  - *Drosophila* genetics and models
  - Intrabody generation
- METHOD DETAILS
  - Drug treatment
  - Immunofluorescence and histology
  - Western and native gel blotting
  - Luminescence measurements
  - Food intake measurements
- QUANTIFICATION AND STATISTICAL ANALYSIS

SUPPLEMENTAL INFORMATION

Supplemental information can be found online at https://doi.org/10.1016/j.crmeth.2022.100292.

ACKNOWLEDGMENTS

Stocks obtained from the Bloomington *Drosophila* Stock Center (NIH P40OD018537) were used in this study. The monoclonal tau antibody 5A6 developed by G.V.W. Johnson was obtained from the Developmental Studies Hybridoma Bank, created by the NICHD of the NIH, and maintained at The University of Iowa, Department of Biology, Iowa City, IA 52242. Special thanks to Jasmine De Mange for assistance with graphic design. This study was supported by the Rainwater Charitable Foundation (S.A.L. and B.F.), NIA T32 AG021890 (G.Z.), NIGMS T32 GM113896 (G.Z.), NCATS TL1 TR002647 (G.Z.), NINDS T32 NS082145 (G.Z.), and NINDS RF1NS123568 (S.T. and D.B.). The graphical abstract and Figure 2A were created using BioRender.com.

AUTHOR CONTRIBUTIONS

Conceptualization, S.A.L. and B.F.; methodology, S.A.L. and B.F.; formal analysis, S.A.L.; investigation, S.A.L, G.Z., and E.M.G.; resources, D.B. and S.T.; writing – original draft, S.A.L.; writing – editing and review, S.A.L., D.B., S.T., and B.F.; visualization, S.A.L. and D.B.; supervision, B.F.; funding acquisition, S.T. and B.F.

DECLARATION OF INTERESTS

The authors declare no competing interests.

INCLUSION AND DIVERSITY

We worked to ensure sex balance in the selection of non-human subjects. One or more of the authors of this paper self-identifies as an underrepresented ethnic minority in science.

Received: March 25, 2022
Revised: July 23, 2022
Accepted: August 17, 2022
Published: September 9, 2022

REFERENCES

Arendt, T., Stieler, J.T., and Holzer, M. (2016). Tau and tauopathies. Brain Res. Bull. *126*, 238–292. https://doi.org/10.1016/j.brainresbull.2016.08.018.

Bardai, F.H., Wang, L., Mutreja, Y., Yenjerla, M., Gamblin, T.C., and Feany, M.B. (2018). A conserved cytoskeletal signaling cascade mediates neurotoxicity of FTDP-17 tau mutations in vivo. J. Neurosci. *38*, 108–119. https://doi.org/10.1523/JNEUROSCI.1550-17.2017.

Beljanski, V. (2007). Radicicol. xPharm: The Comprehensive Pharmacology Reference, 1–3. https://doi.org/10.1016/B978-008055232-3.63582-2.

Von Bergen, M., Barghorn, S., Li, L., Marx, A., Biernat, J., Mandelkow, E.M., and Mandelkow, E. (2001). Mutations of tau protein in frontotemporal dementia promote aggregation of paired helical filaments by enhancing local β-structure. J. Biol. Chem. *276*, 48165–48174. https://doi.org/10.1074/jbc.M105196200.

Braak, H., Thal, D.R., Ghebremedhin, E., and Del Tredici, K. (2011). Stages of the pathologic process in alzheimer disease: age categories from 1 to 100 years. J. Neuropathol. Exp. Neurol. *70*, 960–969. https://doi.org/10.1097/NEN.0b013e318232a379.

Braak, H., and Braak, E. (1991). Neuropathological stageing of Alzheimer-related changes. Acta Neuropathol. *82*, 239–259. https://doi.org/10.1007/BF00308809.

Clavaguera, F., Bolmont, T., Crowther, R.A., Abramowski, D., Frank, S., Probst, A., Fraser, G., Stalder, A.K., Beibel, M., Staufenbiel, M., Jucker, M., Goedert, M., and Tolnay, M. (2009). Transmission and spreading of tauopathy in transgenic mouse brain. Nature Cell Biology *11*, 909–913. https://doi.org/10.1038/ncb1901.

Criado-Marrero, M., Gebru, N.T., Blazier, D.M., Gould, L.A., Baker, J.D., Beaulieu-Abdelahad, D., and Blair, L.J. (2021). Hsp90 co-chaperones, FKBP52 and Aha1, promote tau pathogenesis in aged wild-type mice. Acta Neuropathol. Commun. *9*, 1–16. https://doi.org/10.1186/s40478-021-01159-w.

Frost, B., and Diamond, M.I. (2010). Prion-like mechanisms in neurodegenerative diseases. Nat. Rev. Neurosci. *11*, 155–159. https://doi.org/10.1038/nrn2786.

Frost, B., Jacks, R.L., and Diamond, M.I. (2009a). Propagation of Tau misfolding from the outside to the inside of a cell. J. Biol. Chem. *284*, 12845–12852. https://doi.org/10.1074/jbc.M808759200.

Frost, B., Ollesch, J., Wille, H., and Diamond, M.I. (2009b). Conformational Diversity of Wild-type Tau Fibrils Specified by Templated Conformation Change. Journal of Biological Chemistry *284*, 3546–3551. https://doi.org/10.1074/jbc.M805627200.

Guo, J.L., and Lee, V.M.Y. (2011). Seeding of normal tau by pathological tau conformers drives pathogenesis of Alzheimer-like tangles. J. Biol. Chem. *286*, 15317–15331. https://doi.org/10.1074/jbc.M110.209296.

Han, C., Song, Y., Xiao, H., Wang, D., Franc, N.C., Jan, L.Y., and Jan, Y.N. (2014). Epidermal cells are the primary phagocytes in the fragmentation and clearance of degenerating dendrites in Drosophila. Neuron *81*, 544–560. https://doi.org/10.1016/J.NEURON.2013.11.021.

Hutton, M., Lendon, C.L., Rizzu, P., Baker, M., Froelich, S., Houlden, H., Pickering-Brown, S., Chakraverty, S., Isaacs, A., Grover, A., et al. (1998). Association of missense and 5'-splice-site mutations in tau with the inherited dementia FTDP-17. Nature *393*, 702–705. https://doi.org/10.1038/31508.

Joshi, S.N., Butler, D.C., and Messer, A. (2012). Fusion to a highly charged proteasomal retargeting sequence increases soluble cytoplasmic expression and efficacy of diverse anti-synuclein intrabodies. mAbs *4*, 686–693. https://doi.org/10.4161/mabs.21696.

Karagöz, G.E., Duarte, A.M.S., Akoury, E., Ippel, H., Biernat, J., Moran Luengo, T., Radli, M., Didenko, T., Nordhues, B.A., Veprintsev, D.B., et al. (2014). Hsp90-Tau Complex reveals molecular basis for specificity in chaperone action. Cell *156*, 963–974. https://doi.org/10.1016/J.CELL.2014.01.037.

Krishnaswamy, S., Huang, H.W., Marchal, I.S., Ryoo, H.D., and Sigurdsson, E.M. (2020). Neuronally expressed anti-tau scFv prevents tauopathy-induced phenotypes in Drosophila models. Neurobiol. Dis. *137*, 104770. https://doi.org/10.1016/J.NBD.2020.104770.

Kvam, E., Sierks, M.R., Shoemaker, C.B., and Messer, A. (2010). Physicochemical determinants of soluble intrabody expression in mammalian cell cytoplasm. Protein Eng. Des. Sel. *23*, 489–498. https://doi.org/10.1093/protein/gzq022.

Lewis, J., McGowan, E., Rockwood, J., Melrose, H., Nacharaju, P., Van Slegtenhorst, M., Gwinn-Hardy, K., Paul Murphy, M., Baker, M., Yu, X., et al. (2000). Neurofibrillary tangles, amyotrophy and progressive motor disturbance in mice expressing mutant (P301L)tau protein. Nat. Genet. *25*, 402–405. https://doi.org/10.1038/78078.

Luo, W., Dou, F., Rodina, A., Chip, S., Kim, J., Zhao, Q., Moulick, K., Aguirre, J., Wu, N., Greengard, P., and Chiosis, G. (2007). Roles of heat-shock protein 90 in maintaining and facilitating the neurodegenerative phenotype in tauopathies. Proc. Natl. Acad. Sci. USA *104*, 9511–9516. https://doi.org/10.1073/PNAS.0701055104.

Messer, A., and Butler, D.C. (2020). Optimizing Intracellular Antibodies (Intrabodies/nanobodies) to Treat Neurodegenerative Disorders. In Neurobiology of Disease (Academic Press), p. 104619. https://doi.org/10.1016/j.nbd.2019.104619.

Naik, S., and Piwnica-Worms, D. (2007). Real-time imaging of beta-catenin dynamics in cells and living mice. Proc. Natl. Acad. Sci. USA *104*, 17465–17470. https://doi.org/10.1073/pnas.0704465104.

Patterson, K.R., Remmers, C., Fu, Y., Brooker, S., Kanaan, N.M., Vana, L., Ward, S., Reyes, J.F., Philibert, K., Glucksman, M.J., and Binder, L.I. (2011). Characterization of prefibrillar tau oligomers in vitro and in Alzheimer disease. J. Biol. Chem. *286*, 23063–23076. https://doi.org/10.1074/jbc.M111.237974.

Sanders, D.W., Kaufman, S.K., DeVos, S.L., Sharma, A.M., Mirbaha, H., Li, A., Barker, S.J., Foley, A.C., Thorpe, J.R., Serpell, L.C., et al. (2014). Distinct tau prion strains propagate in cells and mice and define different tauopathies. Neuron *82*, 1271–1288. https://doi.org/10.1016/j.neuron.2014.04.047.

Schneider, C.A., Rasband, W.S., and Eliceiri, K.W. (2012). NIH image to ImageJ: 25 years of image analysis. Nat. Methods *9*, 671–675. https://doi.org/10.1038/NMETH.2089.

Shelton, L.B., Baker, J.D., Zheng, D., Sullivan, L.E., Solanki, P.K., Webster, J.M., Sun, Z., Sabbagh, J.J., Nordhues, B.A., Koren, J., 3rd., et al. (2017). Hsp90 activator Aha1 drives production of pathological tau aggregates. Proc. Natl. Acad. Sci. USA *114*, 9707–9712. https://doi.org/10.1073/pnas.1707039114.

Strang, K.H., Croft, C.L., Sorrentino, Z.A., Chakrabarty, P., Golde, T.E., and Benoit, I.G. (2017). Distinct differences in prion-like seeding and aggregation between Tau protein variants provide mechanistic insights into tauopathies. J. Biol. Chem. *293*, 2408–2421. https://doi.org/10.1074/jbc.M117.815357.

Vaquer-Alicea, J., and Diamond, M.I. (2019). Propagation of protein aggregation in neurodegenerative diseases. Annual Review of Biochemistry *88*, 785–810. https://doi.org/10.1146/annurev-biochem-061516-045049.

Villalobos, V., Naik, S., and Piwnica-Worms, D. (2007). Current state of imaging protein-protein interactions in vivo with genetically encoded reporters. Annu. Rev. Biomed. Eng. *9*, 321–349. https://doi.org/10.1146/annurev.bioeng.9.060906.152044.

Visintin, M., Settanni, G., Maritan, A., Graziosi, S., Marks, J.D., and Cattaneo, A. (2002). The intracellular antibody capture technology (IACT): towards a consensus sequence for intracellular antibodies. J. Mol. Biol. *317*, 73–83. https://doi.org/10.1006/jmbi.2002.5392.

Weickert, S., Wawrzyniuk, M., John, L.H., Rüdiger, S.G.D., and Drescher, M. (2020). The mechanism of Hsp90-induced oligomerizaton of Tau. Sci. Adv. *6*, eaax6999. https://doi.org/10.1126/sciadv.aax6999.

Wittmann, C.W., Wszolek, M.F., Shulman, J.M., Salvaterra, P.M., Lewis, J., Hutton, M., and Feany, M.B. (2001). Tauopathy in Drosophila: neurodegeneration without neurofibrillary tangles. Science *293*, 711–714. https://doi.org/10.1126/science.1062382.

Wolfgang, W.J., Miller, T.W., Webster, J.M., Huston, J.S., Thompson, L.M., Marsh, J.L., and Messer, A. (2005). Suppression of Huntington's disease pathology in Drosophila by human single-chain Fv antibodies. Proc. Natl. Acad. Sci. USA *102*, 11563–11568. https://doi.org/10.1073/pnas.0505321102.

STAR★METHODS

KEY RESOURCES TABLE

REAGENT or RESOURCE	SOURCE	IDENTIFIER
Antibodies		
Tau	Developmental Studies Hybridoma Bank	5A6; RRID: AB_528487
cTau	Dako	A0024; RRID: AB_10013724
EGFP	Invitrogen	CAB4211; RRID: AB_10709851
β-tubulin	Abcam	Ab179513
Alexa Fluor 488 anti-rabbit	Invitrogen	A11008; RRID: AB_143165
Alexa Fluor 555 anti-mouse	Invitrogen	A28180; RRID: AB_2536164
Anti-rabbit human ads-HRP	SouthernBiotech	4010-05; RRID: AB_2632593
Bacterial and virus strains		
pUA plasmid	Han et al., 2014	Addgene 58372; RRID: Addgene_58372
Chemicals, peptides, and recombinant proteins		
Radicicol	Fisher Scientific	55-340-0500UG
DAPI Fluoromount-G	SouthernBiotech	0100–20
D-Luciferin	Thermo Scientific	PI88294
FD & C Blue #1	Fisher Scientific	18-602-610
Critical commercial assays		
TUNEL – FragEL DNA Fragmentation Detection Kit	EMD Millipore	QIA33
SuperSignal West Femto ECL kit	ThermoFisher	34095
Experimental models: Organisms/strains		
elav-Gal4	Bloomington *Drosophila* Stock Center	458; RRID: BDSC_458
w1118	Bloomington *Drosophila* Stock Center	3605; RRID: BDSC_3605
Control: *elav-Gal4/+*	This paper	N/A
Tau^{P301L}: *elav-gal4/+; UAS-*Tau^{P301L}*/+*	This paper	N/A
Tau^{P301L}-NLuc: *elav-gal4/+; UAS-*Tau^{P301L}*-NLuc/+*	This paper	N/A
Tau^{P301L}-CLuc: *elav-gal4/+; UAS-*Tau^{P301L}*-CLuc/+*	This paper	N/A
Tau^{LUM}: *elav-Gal4/+; UAS-*Tau^{P301L}*-NLuc, UAS-*Tau^{P301L}*-CLuc/+*	This paper	N/A
Tau^{LUM} + intrabody: *elav-Gal4/+; UAS-scFv5/+; UAS-*Tau^{P301L}*-NLuc, UAS-*Tau^{P301L}*-CLuc/+*	This paper	N/A
EGFP-NLuc: *elav-gal4/+; UAS-EGFP-NLuc/+*	This paper	N/A
EGFP-CLuc: *elav-gal4/+; UAS-EGFP-CLuc/+*	This paper	N/A
$EGFP^{LUM}$: *elav-Gal4/+; UAS-EGFP-NLuc, UAS-EGFP-CLuc/+*	This paper	N/A
Recombinant DNA		
Tau^{P301L}	This paper	See Table S1
Tau^{P301L}-NLuc	This paper	See Table S1
Tau^{P301L}-CLuc	This paper	See Table S1
EGFP-NLuc	This paper	See Table S1
EGFP-CLuc	This paper	See Table S1
Intrabody scFv5	This paper	See Table S1
Software and algorithms		
GraphPad Prism	GraphPad Software	Prism9; RRID: SCR_002798
ImageJ	Schneider et al., 2012	https://imagej.nih.gov/ij/

RESOURCE AVAILABILITY

Lead contact

Further information and requests for resources and reagents should be directed to and will be fulfilled by the lead contact, Bess Frost (bfrost@uthscsa.edu).

Materials availability

All unique and stable reagents generated in this study are available from the lead contact.

Data and code availability

- All data reported in this paper will be shared by the lead contact upon request.
- This paper does not report original code.
- Any additional information required to reanalyze the data reported in this paper is available from the lead contact upon request.

EXPERIMENTAL MODEL AND SUBJECT DETAILS

Drosophila genetics and models

Drosophila were housed and all crosses were performed at 25°C with a 12h light/dark cycle. Full genotypes are listed in the Key resources table. Pan-neuronal expression of transgenes was achieved using the Gal4/UAS system with the *elav* promoter driving expression of the Gal4 transcription factor. *elav-Gal4 Drosophila* were obtained from the Bloomington *Drosophila* Stock Center (BDSC #458). Plasmids for Tau^{P301L}-NLuc, Tau^{P301L}-CLuc, EGFP-NLuc, EGFP-CLuc, and the anti-tau intrabody scFv5 were generated by GeneWiz and inserted into the pUA vector (Addgene #58372) (Han et al., 2014), which contains ten UAS sequences. *Drosophila* embryo injection of plasmids for PhiC31 integrase-mediated site-specific integration of transgenes was performed by BestGene Inc. NLuc-containing transgenes were inserted at site VK27 (integrase-carrying stock #9744) and CLuc-containing transgenes were inserted at site VK33 (integrase-carrying stock #9759). The intrabody transgene was inserted at site attP1 (integrase-carrying stock #8621) and the tau^{P301L} transgene was inserted at site attP2 (integrase-carrying stock #8622). The sequences for all transgenes used in this study are available in Table S1.

Intrabody generation

GenScript synthesized and codon-optimized the anti-tau single chain fragment variable (scFv) intrabody, #F, originally described by Visintin and colleagues (Visintin et al., 2002). The intrabody was arranged in the following format: Variable heavy chain (VH), flexible linker $(Gly_4Ser)_3$, variable light chain (VL), hemagglutinin (HA) epitope tag, and scrambled inactive PEST degron (ACCGEHPIRPPVEDFEESRASSTASAWLANMVQNKPVSDA). Because many intrabodies suffer from reduced cytoplasmic solubility due to the intracellular redox potential and macromolecular crowding (Kvam et al., 2010; Messer and Butler, 2020), the anti-tau intrabodies were fused to a highly charged proteasomal retargeting sequence to increase soluble cytoplasmic expression and improve intracellular functionality (Joshi et al., 2012).

METHOD DETAILS

Drug treatment

Radicicol was prepared as a 10 mg/mL stock solution in DMSO and diluted in liquid fly food cooled to 60°C to a final concentration of 1 μg/mL. For vehicle controls, an equivalent volume of DMSO was diluted in fly food. *Drosophila* were randomly assigned DMSO or radicicol treatment and placed on drug-containing food from the day of eclosion until the day of measurement.

Immunofluorescence and histology

Drosophila brains were dissected in PBS and fixed for 20 min in methanol. After washing with PBS +0.3% Triton X-100 (PBS-Tr), brains were incubated with blocking buffer (2% w/v milk in PBS-Tr) for 30 min, followed by overnight incubation with primary antibody in blocking buffer at room temperature. After washing with PBS-Tr, brains were incubated with Alexa Fluor conjugated secondary antibody in blocking buffer for 2 h at room temperature. Brains were washed with PBS-Tr again and mounted in DAPI Fluoromount-G (SouthernBiotech #0100-20) to visualize nuclei. Images were acquired by confocal microscopy (Zeiss LSM 880) and analyzed using ImageJ (Schneider et al., 2012).

TUNEL staining was performed using the FragEL DNA Fragmentation Detection Kit (EMD Millipore #QIA33) on 4μm sections of formalin fixed, paraffin embedded *Drosophila* brain tissue. DAB was used to visualize the staining. TUNEL positive nuclei were counted throughout the entire brain by bright-field microscopy.

Western and native gel blotting

For Western blotting, frozen *Drosophila* heads were homogenized in 15μL 2x Laemmli buffer. One head was used per lane. After boiling for 10 min, samples were run on an Any kD Mini-PROTEAN TGX gel (Bio-Rad #4569033) and equal loading of protein was ascertained using Ponceau S staining. For native gel electrophoresis, five frozen *Drosophila* heads per lane were homogenized in 15μL Laemmli buffer. Samples were not boiled and were run on an Any kD Mini-PROTEAN TGX gel in SDS-free running buffer. After blotting, membranes were washed in PBS +0.1% Tween 20 (PBS-Tw) and blocked for 15 min at room temperature in blocking buffer (2% w/v milk + PBS-Tw). Membranes were then incubated with primary antibody diluted in blocking buffer overnight at 4°C on a rocker, washed in PBS-Tw, and incubated with an HRP-conjugated secondary antibody diluted in blocking buffer for 2 h at room temperature. Blots were developed using Super-Signal West Femto ECL kit (ThermoFisher #34095) and band intensities were quantified using ImageJ.

Luminescence measurements

End-point measurements: *Drosophila* were placed on food containing 15mM D-Luciferin (Thermo Scientific #PI88294) in addition to any drug treatments for 24 h. On the day of measurement, flies were anesthetized and transferred to the wells of a 96-well plate. Each well contained one fly. The plate was then covered with a clear plastic adhesive cover (Sigma-Aldrich #Z721417). The flies were left to recover from the anesthesia for 30 min in the plate and transferred to the plate reader, where luminescence signal from each well was integrated for 10 s.

Longitudinal measurements: Live *Drosophila* were placed in 96-well plate wells containing 300μL food with 15mM D-Luciferin. The plate was covered with a clear plastic adhesive cover and small holes were punched above each well to ensure air supply to the animals. The plate was transferred to the plate reader and luminescence signal was integrated for 10 s every hour for two days. The plate was kept in the dark inside the plate reader for the duration of the experiment.

Food intake measurements

On the last day of drug treatment, tau^{LUM} *Drosophila* were placed on food containing 1% (w/v) FD&C Blue #1 dye (Fisher Scientific #18-602-610) along with radicicol or vehicle for 45 min. Five flies were placed in each vial with dyed food. After 45 min, the animals from each vial were frozen, and homogenized in 100μL PBS +1% Triton X-100, and centrifuged briefly to pellet debris. The absorbance of the supernatant at 629nm was then measured with a spectrophotometer. Age-matched flies that were placed on dye-free food served as the baseline absorbance measurement and the amount of ingested food was calculated from a standard curve of serial dilutions of dyed food in PBS +1% Triton X-100.

QUANTIFICATION AND STATISTICAL ANALYSIS

Two-tailed unpaired Student's *t* test was used to compare two means and one-way ANOVA with Dunnett's post-hoc test or two-way ANOVA with Tukey's or Sidak's post-hoc test was used to compare multiple means as appropriate. Exact statistical tests for each graph are listed in figure legends. The experimental unit for all experiments was a single fly. Normality tests indicated that tau^{LUM} and $EGFP^{LUM}$ data were distributed lognormally. We therefore first normalized tau^{LUM} luminescence data to $EGFP^{LUM}$ and then $\log_{10}$ transformed the data. All single time-point luminescence data are presented as $\log_{10}$[luminescence(% of $EGFP^{LUM}$)].